catalysts

MDPI

Article

Pd–Co Nanoparticles Supported on Calcined Mg–Fe Hydrotalcites for the Suzuki–Miyaura Reaction in Water with High Turnover Numbers

Zhenhua Dong [1,*], Pengwei Gao [1], Yongmei Xiao [1], Jing Chen [1,*] and Wentao Wang [2,*]

[1] College of Chemistry and Chemical Engineering, Henan University of Technology, Lianhua Street 100, Zhengzhou 450001, China; chemdzh@163.com (P.G.); chemhaut@foxmail.com (Y.X.)

[2] Dalian Institute of Chemical Physics, Chinese Academy of Sciences, Zhongshan Road 457, Dalian 116023, China

* Correspondence: zhdong@haut.edu.cn (Z.D.); chj-chs@163.com (J.C.); wentaowang@dicp.ac.cn (W.W.); Tel.: +86-0371-67756718 (Z.D. & J.C.); +86-136-6300-3280 (W.W.)

Received: 20 November 2019; Accepted: 10 December 2019; Published: 13 December 2019

Abstract: We reveal the Suzuki–Miyaura reaction catalyzed by a Pd–Co nanocatalyst supported by Mg–Fe–CHT (calcined hydrotalcites). A variety of boronic acids and aryl halides were transformed into functionalized biphenyls in excellent yields using water as a solvent. The reaction could proceed under mild conditions with a simple operation and high turnover numbers. The excellent catalytic activities are reasonably attributed to the Co-doping, which forms a Pd–Co alloy on the surface of CHT.

Keywords: Suzuki–Miyaura reaction; water solvent; nanocatalyst; palladium; cobalt

1. Introduction

In the past decades, carbon–carbon cross couplings have been widely applied for the synthesis of natural products and biologically active molecules [1–4]. Among them, the Suzuki–Miyaura reaction is one of the most versatile and significant methods [5–7]. Numerous highly active homogeneous Pd catalytic systems have been investigated for the reaction [8–12]. However, the use of homogeneous Pd catalysts incurs a high cost due to the utilization of unrecoverable noble metals and ligands. In addition, practical limitations, such as catalyst operation, reusability, and isolation of the catalyst from products, hinder the advantages of homogeneous Pd catalysts in large-scale industrial processes. By contrast, a heterogeneous Pd catalyst could obviate these limitations and open up a valuable alternative technology in such processes [13–17]. In recent years, palladium nanoparticles (NPs) supported by various substrates, such as active carbon materials [18,19], silica [20–22], polymers [23,24], inorganic mineral [25,26], metal oxides [27–29], and covalent organic frameworks (COFs) [30,31] have been designed and applied for the Suzuki–Miyaura reaction. However, these methods usually require high catalyst loadings (from 0.021 to 1 mol % Pd), high-reaction temperatures, and long reaction times. Interested authors may find further information in Table S1 of the Supplementary Materials accompanying this paper. As a result, there is still great potential for improving the catalyst performance. The development of new and more efficient catalysts for the Suzuki–Miyaura reaction, which are highly active and perform well under environmentally friendly reaction conditions, is highly desirable. Hence, we report a novel catalyst consisting of Pd–Co nanoparticles supported by Mg–Fe–CHT (calcined hydrotalcites) [32–38] and its application in the Suzuki–Miyaura reaction under green conditions, with a TON (turnover numbers) value up to 42,609. The reaction was carried out in water under atmospheric conditions.

2. Results and Discussion

The preparation of the Pd/Co–Mg–Fe–CHT catalyst is shown in Scheme 1 via a co-precipitation method. Using the analogous operation, we also prepared Mg–Fe–CHT and Co–Mg–Fe–CHT. In our initial evaluation of the Suzuki–Miyaura coupling condition, iodobenzene and phenylboronic acid were used as model substrates with two equivalents of base and 10 mg Pd or Co nanoparticles (NPs) prepared by various methods (Supplementary Materials) [39–41]. We found that the Pd-NPs supported by Mg–Fe–CHT could promote the coupling reaction with 93% yield (Table 1, Entry 1). With a view to recycle the catalyst, we prepared Pd-doped Co-NPs supported by Mg–Fe–CHT. The inductively coupled plasma (ICP) analysis showed that the Pd and Co content in calcined hydrotalcite is 0.49 wt % and 0.67 wt %, respectively.

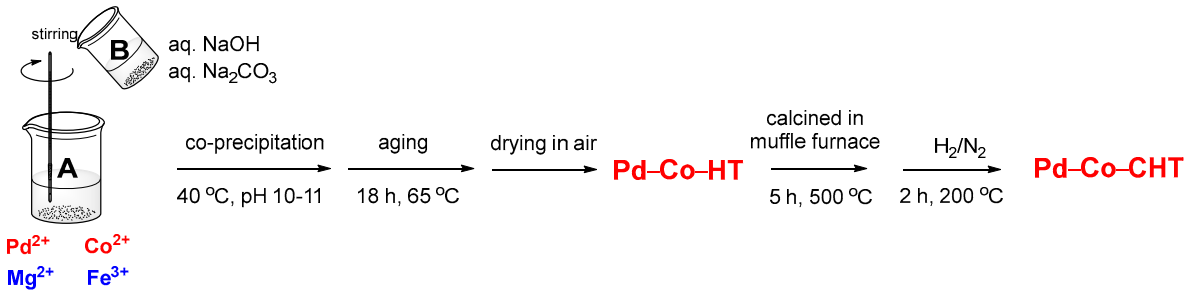

Scheme 1. Preparation of Pd–Co–Mg–Fe–CHT.

Table 1. The optimization of the Suzuki coupling catalyzed by various metal nanoparticles [a].

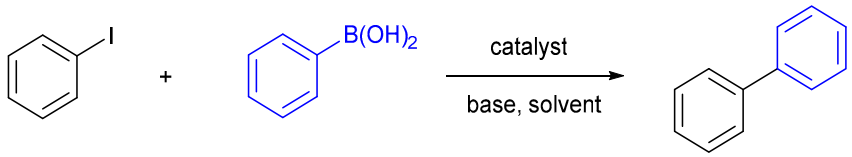

1a 2a 3a

Entry	Catalyst	Solvent	Base	Temp (°C)	Yield [b]
1	Pd–CHT [d]	DMSO	K_2CO_3	110	93%
2	Pd–Co–CHT	DMSO	K_2CO_3	110	99%
3	Co–CHT	DMSO	K_2CO_3	110	0%
4	CHT	DMSO	K_2CO_3	110	0%
5	Pd–Co–CHT	DMF	K_2CO_3	110	98%
6	Pd–Co–CHT	toluene	K_2CO_3	100	92%
7	Pd–Co–CHT	water	K_2CO_3	80	99%
8	Pd–Co–CHT	water	-	80	0%
9 [c]	Pd–Co–CHT	water	K_2CO_3	80	99%
10	Pd–CHT	water	K_2CO_3	80	94%
11	Pd–Co–CHT	water	K_2CO_3	60	90%

[a.] Iodobenzene (5 mmol), phenyl boronic acids (7.5 mmol), K_2CO_3 (10 mmol), Pd–Co–Mg–Fe–CHT (9 mmol % Pd, 10.0 mg), solvent (5.0 mL) for 6 h; [b.] isolated yield; [c.] Pd–Co–CHT (5 mmol % Pd, 5.0 mg), 12 h; [d.] CHT = Mg–Fe–CHT.

When Pd–Co–Mg–Fe–CHT was used as the catalyst, there was complete conversion to biphenyl (Table 1, Entry 2). In contrast, the sole Mg–Fe–CHT and Co-NPs supported by Mg–Fe–CHT had no catalytic activity (Table 1, Entries 3 and 4). Then, several solvents were screened, and excellent yields were also obtained by using DMF and toluene as the solvent (Table 1, Entries 5 and 6). To our delight, the coupling could be promoted in water with 99% yield at 80 °C in 6 h (Table 1, Entry 7). Succeeding experiments revealed that that the base (K_2CO_3) was essential (Table 1, Entry 8). We then attempted to reduce the amount of NPs utilized to 5 mg. The results revealed that a complete transformation needed longer reaction times (Table 1, Entry 9). Considering the low loading of metal in calcined

hydrotalcite, the 10 mg Pd–Co–Mg–Fe–CHT-NPs were acceptable. Under optimized conditions, the Pd catalyst loading could be as low as 0.009 mol % with a TON value up to 10,761. The catalytic capacity of sole Pd–Mg–Fe–CHT in water was also tested. The yield was decreased appreciably compared with Pd–Co–Mg–Fe–CHT (Table 1, Entry 10). The results of temperature screening showed that low temperature was not sufficient (Table 1, Entry 11).

Under optimized reaction conditions, various aryl halides and boronic acids were tested. It was observed that Pd–Co–Mg–Fe–CHT works efficiently with electron withdrawing and electron donating substituents on boronic acid such as -OMe, -F, and -COMe (Table 2, Entry 1–5). However, the bromobenzene gave moderate yield (Table 2, Entry 6). For the chloro- and fluoro-substituted substrates, excellent yields could be achieved with complete chemoselectivity (Table 2, Entry 7–9). A series of other aryl iodides with different electronic characters and steric effects were also measured, and excellent isolated yields were obtained (Table 2, Entries 10–17). The reaction also proceeded with fused ring aryl iodide to provide the corresponding product with 83% yield (Table 2, Entry 18).

Table 2. Substrate Scope [a].

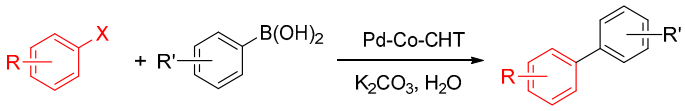

1 **2** **3**

Entry	Aryl Halides	Boronic Acid	Product	Yield [b]
1	PhI	3,4-DiMeO-$C_6H_4B(OH)_2$	**3b**	90
2	PhI	3-MeO-$C_6H_4B(OH)_2$	**3c**	97
3	PhI	4-MeO-$C_6H_4B(OH)_2$	**3d**	99
4	PhI	4-F-$C_6H_4B(OH)_2$	**3e**	94
5	PhI	4-CH_3CO-$C_6H_4B(OH)_2$	**3f**	92
6	PhBr	$PhB(OH)_2$	**3a**	52
7	4-Cl-C_6H_4I	$PhB(OH)_2$	**3g**	99
8	4-F-C_6H_4I	$PhB(OH)_2$	**3h**	99
9	3-Cl-C_6H_4I	$PhB(OH)_2$	**3i**	99
10	4-CH_3CO-C_6H_4I	$PhB(OH)_2$	**3f**	97
11	4-*t*Bu-C_6H_4I	$PhB(OH)_2$	**3j**	99
12	4-MeO-C_6H_4I	$PhB(OH)_2$	**3d**	98
13	3-MeO-C_6H_4I	$PhB(OH)_2$	**3c**	97
14	3,4-DiMe-C_6H_3I	$PhB(OH)_2$	**3k**	99
15	4-Me-C_6H_4I	$PhB(OH)_2$	**3l**	99
16	3-Me-C_6H_4I	$PhB(OH)_2$	**3m**	99
17	2-Me-C_6H_4I	$PhB(OH)_2$	**3n**	94
18	1-Iodonaphthal	$PhB(OH)_2$	**3o**	83

[a] Reaction conditions: aryl halides (5 mmol), boronic acids (7.5 mmol), K_2CO_3 (10 mmol), Pd–Co–Mg–Fe–CHT (10 mg, 0.009 mol % Pd), water (5 mL) at 80 °C for 6 h. [b] Isolated yields.

Furthermore, biphenyl product could be provided by gram-scale synthesis successfully (Scheme 2). The dosages of raw material were expanded to 20 times with lower catalyst loading. A total of 15.1 g biphenyl could produce a 98% yield with a TON value up to 42,609.

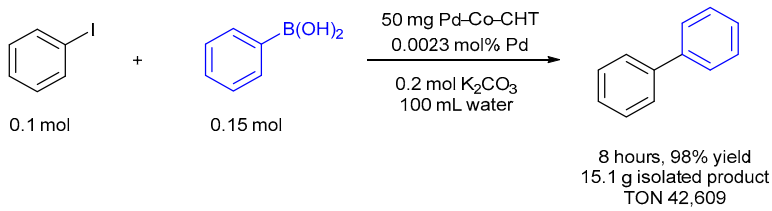

Scheme 2. Gram-scale reaction for the synthesis of biphenyl.

For the recycling test of Pd–Co–Mg–Fe–CHT, a reaction of iodobenzene with phenylboronic acid was conducted under optimized reaction conditions for 6 h (Scheme 3). After the reaction, the Pd–Co catalyst was easily separated by magnetic separation or by simple filtration (see Figure S1), washed by water and diethyl ether, and dried. Another run was conducted subsequently. The catalyst could be easily separated by magnetic decantation and exhibited good recyclability and stability. Pd–Co–Mg–Fe–CHT could be used successively three times without any significant loss of catalytic activity.

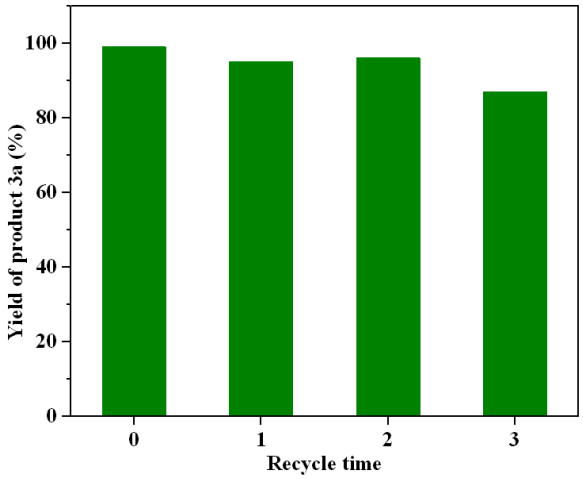

Scheme 3. The reuse experiments.

The Pd–Co–HT and Pd–Co–CHT powders were analyzed by powder X-ray diffraction (XRD) (see Figure S2 in the Supplementary Materials). The XRD patterns of Pd–Co–HT exhibited the typical peaks of HT with symmetric and sharp reflections for the (003), (006), (110), and (113) planes. In addition, asymmetric and wide reflections were assigned to the (012), (015), and (018) planes, revealing the characteristics of hydrotalcite-like compounds. Pd–Co–CHT exhibiting mixed oxide (Mg (Fe) O) was formed, corresponding to the peaks at 43° and 62°. The surface area of Pd–Co–CHT is 77.23 m^2/g for the CHT, which has a mesoporous structure with an average pore size of more than 2 nm.

Figure 1a and Figure S3 show the TEM images of Pd–Co–CHT. It can be seen that Pd–Co nanoparticles are unevenly dispersed in the lamellar structure of CHT. Figure 1c,d shows the HRTEM images of the selected regions in Figure 1b, which contain Pd–Co nanoparticles with the d spacing of the (111) plane. The corresponding d values in Figure 1c,d are d = 0.224 nm and d = 0.228 nm, respectively. Figure 1e,f was obtained by inverse FFT images of Figure 1c,d, and significant anti-site defects can be seen in both plots. Both Pd and Co are face-centered cubic structures (Fm-3m). The (111) plane spacing of crystal Pd is d = 0.225 nm (JCPDF46-1043), and the (111) plane spacing of Co is d = 0.197 nm (JCPDF88-2325). The reason for the anti-site defect is probably due to the doping of Co, which locally forms a Pd–Co alloy on the CHT.

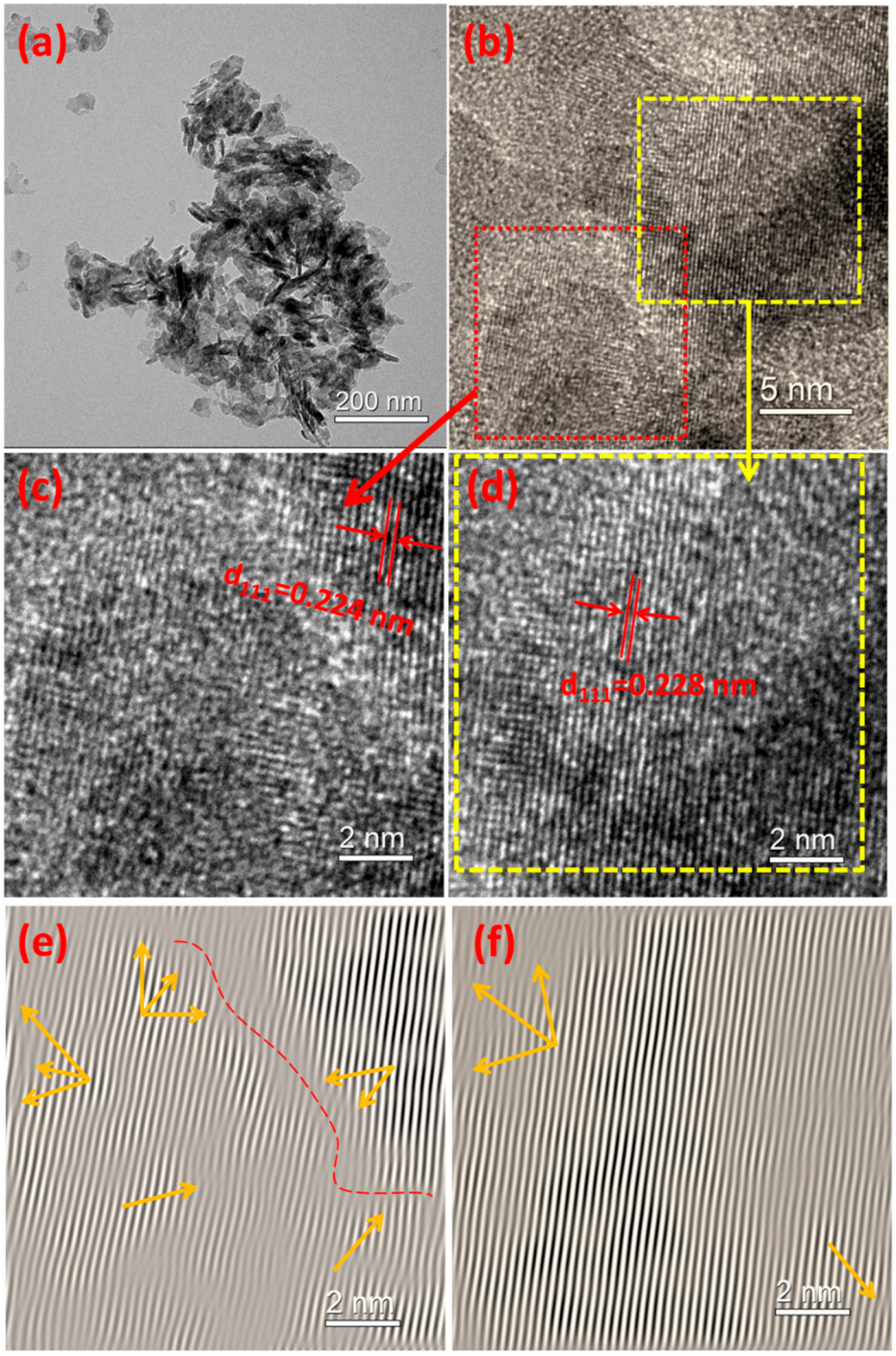

Figure 1. (**a**,**b**) HRTEM images of the Pd–Co–CHT powder. (**c**,**d**) are magnified images of the selected areas of red and yellow squares in (b). (**e**,**f**) are inverse FFT images of (c) and (d), along with anti-site defects marked with arrows.

As can be seen from Table 1, the yield of the Suzuki coupling using the Pd–CHT catalyst was 93%, and the yield went up to 99% after the Co-doping of the Pd–Co–CHT catalyst. Therefore, we believe that the Co-doping, which forms the Pd–Co alloy on the surface of the CHT, causes the Pd to have a reverse defect. This defect increases the reactive site of Pd, prompting the Suzuki coupling reaction to proceed efficiently.

3. Materials and Methods

3.1. General Method

All reagents were of analytical grade and purchased from Aladdin Industrial Inc. (Shanghai, China). NMR spectrograms were recorded on a 400 MHz spectrometer. TEM images were characterized by a JEOL 2100F instrument (Tokyo, Japan). ICP-AES (Inductively Coupled Plasma Atomic Emission Spectroscopy) was tested by an IRIS Intrepid II XSP instrument (Thermo Electron Corp., Waltham, MA, USA). XRD was collected on a D8 Advance using Cu Kα radiation from 5 to 80° (2θ).

3.2. Synthesis of Pd–Co–CHT

Pd/Co–HT with a ratio of Mg/Fe = 3 was prepared by a co-precipitation method. The two solutions, A and B, were synchronously added into deionized water (100 mL) dropwise, with vigorous stirring. Solution A (200 mL) contained $MgCl_2{\cdot}6H_2O$ (1.2 mol/L), $FeCl_3{\cdot}6H_2O$ (0.4 mol/L), $PdCl_2$ (7.5×10^{-3} mol/L), and $CoCl_2$ (1.4×10^{-2} mol/L). Solution B (200 mL) contained enough NaOH and Na_2CO_3 to precipitate solution A completely. The co-precipitation temperature was carried out at 40 °C, while the pH was kept constant at 10–11 by adding NaOH. Then, the precipitate was aged for 18 h at 65 °C to obtain the final solid. Next, the solid was washed by centrifuge with deionized water several times until the specific conductance of the supernate was below 300 μs/cm. The solid was dried for 8 h at 105 °C in air, and the product was denoted as Pd–Co–HT. The Pd–Co–HT products were calcined at 500 °C for 5 h in a muffle furnace. The powder was reduced for 2 h at 200 °C under flowing H_2 and N_2 (flow rate: 50/150 mL/min). The final powder was named Pd–Co–CHT.

3.3. General Procedure for the Suzuki–Miyaura Coupling Catalyzed by Pd–Co–CHT

Boronic acids (7.5 mmol), aryl halide (5.0 mmol), K_2CO_3 (10 mmol), and 10 mg of the Pd–Co–Mg–Fe–CHT (9 mmol % Pd, 22.8 mmol % Co) nanocatalyst were added in water (5 mL), and the reaction proceeded at 80 °C for 6 h. The reaction was monitored by TLC (Thin layer chromatography). After reaction completion, the catalyst was separated by filtration, and the filtrate was extracted with diethyl ether. The catalyst could be easily recovered by simple filtration or by magnetic separation, washed by water and diethyl ether, and dried for subsequent runs. The products were isolated by column chromatography (petroleum ether as eluent). The recyclability study was run subsequently using the recovered catalyst. The products were characterized by ^{1}HNMR and MS.

4. Conclusions

In summary, an environmentally friendly method for the Suzuki cross coupling of aryl halides and boronic acids was developed using a Pd–Co–CHT nanocatalyst under mild conditions in water solvent. A variety of aryl halides and boronic acids with several functional groups progressed well. This protocol has several advantages, such as low loading of catalyst (0.009 mol %), an outstanding TON value (10,761), and use of a cheap and green solvent (water). By using optimized conditions, the Pd–Co–CHT catalyst could be recycled up to three times without a significant loss in catalytic activity. The coupling could proceed with this scale up to 15 g with a low 0.0023 mol % catalyst loading and a 42,609 TON value.

Supplementary Materials: The following are available online at http://www.mdpi.com/2073-4344/9/12/1061/s1, Figure S1: Magnetic separation of the catalyst. Figure S2: Typical XRD patterns of Pd–Co–HT, Pd–Co–CHT. Figure S3: HRTEM image of the Pd–Co–CHT powder. Table S1: Comparison between previous reported works and the present work for Suzuki coupling reaction of aryl halide with phenyl boronic acid.

Author Contributions: Z.D. contributed to the experiment design, article writing, and editing. P.G. and Y.X. contributed to all the experimental data collection. J.C. and W.W. contributed to product analyses, as well as helpful discussion.

Funding: The authors are grateful to the Doctor Fund of Henan University of Technology (No. 2015BS013), State Key Laboratory of Materials Processing and Die & Mould Technology, Huazhong University of Science and

Technology (No. P2019-004), Key Specialized R&D Breakthrough-Scientific and Technological Research Project in Henan Province (No. 192102210170), and Key Scientific and Technological Research Projects of Henan Education Committee (No. 14B430005).

Conflicts of Interest: The authors declare no conflicts of interest.

References

1. Schwan, A.L. Palladium catalyzed cross-coupling reactions for phosphorus-carbon bond formation. *Chem. Soc. Rev.* **2004**, *33*, 218–224. [CrossRef] [PubMed]
2. Terao, J.; Kambe, N. Cross-Coupling Reaction of Alkyl Halides with Grignard Reagents Catalyzed by Ni, Pd, or Cu Complexes with pi-Carbon Ligand(s). *Acc. Chem. Res.* **2008**, *41*, 1545–1554. [CrossRef] [PubMed]
3. Bariwal, J.; Van der Eycken, E. C-N bond forming cross-coupling reactions: An overview. *Chem. Soc. Rev.* **2013**, *42*, 9283–9303. [CrossRef] [PubMed]
4. Zhang, Y.-F.; Shi, Z.-J. Upgrading Cross-Coupling Reactions for Biaryl Syntheses. *Acc. Chem. Res.* **2019**, *52*, 161–169. [CrossRef] [PubMed]
5. Hussain, I.; Capricho, J.; Yawer, M.A. Synthesis of Biaryls via Ligand-Free Suzuki-Miyaura Cross-Coupling Reactions: A Review of Homogeneous and Heterogeneous Catalytic Developments. *Adv. Synth. Catal.* **2016**, *358*, 3320–3349. [CrossRef]
6. Beletskaya, I.P.; Alonso, F.; Tyurin, V. The Suzuki-Miyaura reaction after the Nobel prize. *Coord. Chem. Rev.* **2019**, *385*, 137–173. [CrossRef]
7. Hooshmand, S.E.; Heidari, B.; Sedghi, R.; Varma, R.S. Recent advances in the Suzuki-Miyaura cross-coupling reaction using efficient catalysts in eco-friendly media. *Green Chem.* **2019**, *21*, 381–405. [CrossRef]
8. Pereira, R.; Iglesias, B.; de Lera, A.R. Regioselective palladium-catalyzed cross-coupling reactions in the synthesis of novel 2,3-disubstituted thiophene derivatives. *Tetrahedron* **2001**, *57*, 7871–7881. [CrossRef]
9. Denmark, S.E.; Yang, S.M. Sequential ring-closing metathesis/Pd-catalyzed, Si-assisted cross-coupling reactions: General synthesis of highly substituted unsaturated alcohols and medium-sized rings containing a 1,3-cis-cis diene unit. *Tetrahedron* **2004**, *60*, 9695–9708. [CrossRef]
10. So, C.M.; Kwong, F.Y. Palladium-catalyzed cross-coupling reactions of aryl mesylates. *Chem. Soc. Rev.* **2011**, *40*, 4963–4972. [CrossRef]
11. Han, F.-S. Transition-metal-catalyzed Suzuki-Miyaura cross-coupling reactions: A remarkable advance from palladium to nickel catalysts. *Chem. Soc. Rev.* **2013**, *42*, 5270–5298. [CrossRef] [PubMed]
12. Kinney, R.G.; Tjutrins, J.; Torres, G.M.; Liu, N.J.B.; Kulkarni, O.; Arndtsen, B.A. A general approach to intermolecular carbonylation of arene C-H bonds to ketones through catalytic aroyl triflate formation. *Nat. Chem.* **2018**, *10*, 193–199. [CrossRef] [PubMed]
13. Karimi, B.; Mansouri, F.; Mirzaei, H.M. Recent Applications of Magnetically Recoverable Nanocatalysts in C-C and C-X Coupling Reactions. *ChemCatChem* **2015**, *7*, 1736–1789. [CrossRef]
14. Baeza, A.; Guillena, G.; Ramón, D.J. Magnetite and Metal-Impregnated Magnetite Catalysts in Organic Synthesis: A Very Old Concept with New Promising Perspectives. *ChemCatChem* **2016**, *8*, 49–67. [CrossRef]
15. Nasrollahzadeh, M.; Issaabadi, Z.; Tohidi, M.M.; Sajadi, S.M. Recent Progress in Application of Graphene Supported Metal Nanoparticles in C-C and C-X Coupling Reactions. *Chem. Rec.* **2018**, *18*, 165–229. [CrossRef]
16. Hui, Y.H.; Zhang, S.W.; Wang, W.T. Recent Progress in Catalytic Oxidative Transformations of Alcohols by Supported Gold Nanoparticles. *Adv. Synth. Catal.* **2019**, *361*, 2215–2235. [CrossRef]
17. Dong, Z.; Yuan, J.; Xiao, Y.; Mao, P.; Wang, W. Room Temperature Chemoselective Deoxygenation of Aromatic Ketones and Aldehydes Promoted by a Tandem Pd/TiO2 + FeCl3 Catalyst. *J. Org. Chem.* **2018**, *83*, 11067–11073. [CrossRef]
18. Suresh Kumar, B.; Amali, A.J.; Pitchumani, K. Fabrication of Pd Nanoparticles Embedded C@Fe3O4 Core-Shell Hybrid Nanospheres: An Efficient Catalyst for Cyanation in Aryl Halides. *ACS Appl. Mater. Interfaces* **2015**, *7*, 22907–22917. [CrossRef]
19. Li, D.D.; Zhang, J.W.; Cai, C. Pd Nanoparticles Supported on Cellulose as a Catalyst for Vanillin Conversion in Aqueous Media. *J. Org. Chem.* **2018**, *83*, 7534–7538. [CrossRef]
20. Ghorbani-Choghamarani, A.; Nikpour, F.; Ghorbani, F.; Havasi, F. Anchoring of Pd(ii) complex in functionalized MCM-41 as an efficient and recoverable novel nano catalyst in C–C, C–O and C–N coupling reactions using Ph3SnCl. *RSC Adv.* **2015**, *5*, 33212–33220. [CrossRef]

21. Saha, A.; Wu, C.-M.; Peng, R.; Koodali, R.; Banerjee, S. Facile Synthesis of 1,3,5-Triarylbenzenes and 4-Aryl-NH-1,2,3-Triazoles Using Mesoporous Pd-MCM-41 as Reusable Catalyst. *Eur. J. Org. Chem.* **2019**, *2019*, 104–111. [CrossRef]
22. Khazaei, A.; Khazaei, M.; Nasrollahzadeh, M. Nano-Fe3O4@SiO2 supported Pd(0) as a magnetically recoverable nanocatalyst for Suzuki coupling reaction in the presence of waste eggshell as low-cost natural base. *Tetrahedron* **2017**, *73*, 5624–5633. [CrossRef]
23. da Costa, A.P.; Nunes, D.R.; Tharaud, M.; Oble, J.; Poli, G.; Rieger, J. Palladium(0) Nanoparticles Embedded in Core-shell Nanogels as Recoverable Catalysts for the Mizoroki-Heck Reaction. *ChemCatChem* **2017**, *9*, 2167–2175. [CrossRef]
24. Guo, B.; Li, H.X.; Zha, C.H.; Young, D.J.; Li, H.Y.; Lang, J.P. Visible-Light-Enhanced Suzuki-Miyaura Reactions of Aryl Chlorides in Water with Pd NPs Supported on a Conjugated Nanoporous Polycarbazole. *ChemSusChem* **2019**. [CrossRef] [PubMed]
25. Farhang, Y.; Taheri-Nassaj, E.; Rezaei, M. Pd doped LaSrCuO4 perovskite nano-catalysts synthesized by a novel solid state method for CO oxidation and Methane combustion. *Ceram. Int.* **2018**, *44*, 21499–21506. [CrossRef]
26. Koizumi, Y.; Jin, X.; Yatabe, T.; Miyazaki, R.; Hasegawa, J.Y.; Nozaki, K.; Mizuno, N.; Yamaguchi, K. Selective Synthesis of Primary Anilines from NH3 and Cyclohexanones by Utilizing Preferential Adsorption of Styrene on the Pd Nanoparticle Surface. *Angew. Chem.* **2019**. [CrossRef] [PubMed]
27. Shelkar, R.S.; Gund, S.H.; Nagarkar, J.M. Nano Pd–Fe3O4@Alg beads: As an efficient and magnetically separable catalyst for Suzuki, Heck and Buchwald–Hartwig coupling reactions. *RSC Adv.* **2014**, *4*, 53387–53396. [CrossRef]
28. Zhang, J.; Xie, B.; Wang, L.; Yi, X.F.; Wang, C.T.; Wang, G.X.; Dai, Z.F.; Zheng, A.M.; Xiao, F.S. Zirconium Oxide Supported Palladium Nanoparticles as a Highly Efficient Catalyst in the Hydrogenation-Amination of Levulinic Acid to Pyrrolidones. *ChemCatChem* **2017**, *9*, 2661–2667. [CrossRef]
29. Chatterjee, T.; Dey, R.; Ranu, B.C. ZnO-supported Pd nanoparticle-catalyzed ligand- and additive-free cyanation of unactivated aryl halides using $K_4[Fe(CN)_6]$. *J. Org. Chem.* **2014**, *79*, 5875–5879. [CrossRef]
30. Sadhasivam, V.; Balasaravanan, R.; Chithiraikumar, C.; Siva, A. Palladium Nanoparticles Supported on Nitrogen-rich Containing Melamine-based Microporous Covalent Triazine Polymers as Efficient Heterogeneous Catalyst for C-Se Coupling Reactions. *ChemCatChem* **2018**, *10*, 3833–3844. [CrossRef]
31. Lu, S.; Hu, Y.; Wan, S.; McCaffrey, R.; Jin, Y.; Gu, H.; Zhang, W. Synthesis of Ultrafine and Highly Dispersed Metal Nanoparticles Confined in a Thioether-Containing Covalent Organic Framework and Their Catalytic Applications. *J. Am. Chem. Soc.* **2017**, *139*, 17082–17088. [CrossRef] [PubMed]
32. Meng, X.; Bi, X.; Yu, C.; Chen, G.; Chen, B.; Jing, Z.; Zhao, P. Ball-milling synthesized hydrotalcite supported Cu–Mn mixed oxide under solvent-free conditions: An active catalyst for aerobic oxidative synthesis of 2-acylbenzothiazoles and quinoxalines. *Green Chem.* **2018**, *20*, 4638–4644. [CrossRef]
33. Wang, Y.B.; Yu, K.; Lei, D.; Si, W.; Feng, Y.J.; Lou, L.L.; Liu, S.X. Basicity-Tuned Hydrotalcite-Supported Pd Catalysts for Aerobic Oxidation of 5-Hydroxymethyl-2-furfural under Mild Conditions. *ACS Sustain. Chem. Eng.* **2016**, *4*, 4752–4761. [CrossRef]
34. Karanjit, S.; Kashihara, M.; Nakayama, A.; Shrestha, L.K.; Ariga, K.; Namba, K. Highly active and reusable hydrotalcite-supported Pd(0) catalyst for Suzuki coupling reactions of aryl bromides and chlorides. *Tetrahedron* **2018**, *74*, 948–954. [CrossRef]
35. Burrueco, M.I.; Mora, M.; Jiménez-Sanchidrián, C.; Ruiz, J.R. Hydrotalcite-supported palladium nanoparticles as catalysts for the Suzuki reaction of aryl halides in water. *Appl. Catal. A Gen.* **2014**, *485*, 196–201. [CrossRef]
36. Jin, X.; Koizumi, Y.; Yamaguchi, K.; Nozaki, K.; Mizuno, N. Selective Synthesis of Primary Anilines from Cyclohexanone Oximes by the Concerted Catalysis of a Mg-Al Layered Double Hydroxide Supported Pd Catalyst. *J. Am. Chem. Soc.* **2017**, *139*, 13821–13829. [CrossRef] [PubMed]
37. Comelli, N.A.; Ruiz, M.L.; Merino, N.A.; Lick, I.D.; Rodriguez-Castellon, E.; Jimenez-Lopez, A.; Ponzi, M.I. Preparation and characterisation of calcined Mg/Al hydrotalcites impregnated with alkaline nitrate and their activities in the combustion of particulate matter. *Appl. Clay Sci.* **2013**, *80*, 426–432. [CrossRef]
38. Ruiz, J.R.; Jiménez-Sanchidrián, C.; Mora, M. Suzuki cross-coupling reaction of fluorobenzene with heterogeneous palladium catalysts. *J. Fluor. Chem.* **2006**, *127*, 443–445. [CrossRef]

39. Shaabani, A.; Hezarkhani, Z.; Nejad, M.K. AuCu and AgCu bimetallic nanoparticles supported on guanidine-modified reduced graphene oxide nanosheets as catalysts in the reduction of nitroarenes: Tandem synthesis of benzo[b][1,4]diazepine derivatives. *RSC Adv.* **2016**, *6*, 30247–30257. [CrossRef]
40. Dhital, R.N.; Kamonsatikul, C.; Somsook, E.; Bobuatong, K.; Ehara, M.; Karanjit, S.; Sakurai, H. Low-temperature carbon-chlorine bond activation by bimetallic gold/palladium alloy nanoclusters: An application to Ullmann coupling. *J. Am. Chem. Soc.* **2012**, *134*, 20250–20253. [CrossRef]
41. Antony, R.; Marimuthu, R.; Murugavel, R. Bimetallic Nanoparticles Anchored on Core–Shell Support as an Easily Recoverable and Reusable Catalytic System for Efficient Nitroarene Reduction. *ACS Omega* **2019**, *4*, 9241–9250. [CrossRef] [PubMed]